EE3L11 BAP
Literature Study
Subgroup: Phantom

April 26, 2022

Bogaert, B. 5107105
Mijjer, L. 4727207
Otter, M. 4771184

TU Delft

Contents

1

Literature Study

For the bachelor end project (BAP), a phantom needs to be made to act as a test ground for the design of a brain computer interface (BCI). Phantoms are objects that mimic or imitate the dielectric properties of human tissues, like skin. Phantoms are used to evaluate, analyze and tune the performance of medical devices. For this particular case, a phantom will be used to evaluate and analyze the performance of a dry surface electrode. This electrode will be the interface/bridge for signals travelling between the computer device and human skin (and indirectly the brain). A phantom is chosen over living tissues because of safety reasons, it is more readily available and provides consistent results.

In order to model/create a phantom that mimics the nature of human skin, some background knowledge is required. Such material is given below.

1.1. Materials/composition of phantom

The phantom needs to be made by material that closely resembles human skin. Gelatin is an excellent choice for this since it is made from animal products. Gelatin is easy available, nontoxic, low cost, and allows easy modeling of the phantom's shape [2]. Thus, it can be ideal as a test ground for dry electrode measurements and experiments. The phantom ear can be copied in gelatin from a 3D-printed mold.

Figure 2.1 shows the relation between frequency and impedance for gelatine in the range from 1 to 10 MHz. It is visible that the impedance exponentially increases when the frequency decreases. The phantoms with higher concentration of gelatin have a higher impedance.

Figure 2.2 shows the same relation but now when the gelatine is prepared with salt content. The addition of salt to gelatins induces profound changes in the impedance modulus profile [2]. The addition of salt lowers the impedance quite significantly.

Figure 2.3 shows the relation between the impedance and gelatin/salt concentrations.

These relations can be used in the production of a gelatin ear phantom to closely model the real human ear. By altering the concentration of NaCl, the electrical properties of the skin phantom can be adjusted such that the phantom mimics real human skin, as shown by [28].

1.2. Dielectric properties

The dielectric properties of materials are obtained from their measured complex relative permittivity, $\hat{\epsilon}$ expressed as

$$\hat{\epsilon} = \epsilon' - j\epsilon'' \tag{1.1}$$

$$\epsilon'' = \frac{\sigma}{\epsilon_0 \omega} \tag{1.2}$$

ϵ' is the relative permittivity of the material and ϵ'' is the out-of-phase loss factor associated with Equation 1.2, where σ is the total conductivity of the material. ϵ_0 is the permittivity of free space and ω the angular frequency of the field [4].

The impedance of the skin is an important factor as this defines how much power needs to be delivered from the transmitting to the receiving probe to make a meaningful analysis and it follows following equation, where ω is the radial frequency:

$$Z(\omega) = V(\omega)/I(\omega) \tag{1.3}$$

Since, the whole circuit needs to be inside an earpiece, it is recommended to work with low power and this requires a low impedance since the relation between voltage is linear. The study of dry electrodes showed a mean impedance of the canal electrodes of 1.2MΩ [13]. However, the measurements also showed high variations in the impedance, leading to impedance mismatch between the electrodes, demanding a high input impedance to avoid a significant drop in the common mode rejection ratio (CMRR) of the system.

1.3. Electrode-skin interface

Living cells and tissues of human beings and animals generate electric signals. These are also often referred to as bioelectrical signals. These signals reflect the physiological state of organs and/or tissues and it is therefore important to have the ability of detecting these signals. In such a detection process, an electrode is used as a tool to conduct/transport bioelectrical signals to a detection device such that these signals can be analyzed. As mentioned at the start of this chapter, the phantom will be mainly used to analyze the performance of a dry surface electrode. Therefore, it is necessary to know the layered structure of skin and the electrode-skin interface, such that the phantom can be appropriately modelled to mimic human skin.

1.3.1. General Case: Wet Surface Electrodes

The clinical standard are Ag/AgCl wet electrodes [19], where, generally, a conductive gel is applied between the skin and the electrode to improve the conductivity between the interface of the two. The interaction between human skin and wet electrode (/electric coupling) can be be described as a layered conductive and capacitive structure, with a material dependent number of parallel RC elements connected in series. This is visualized by the simplified equivalent circuit shown in Figure 1.1 [8, 19]. The left side of the Figure shows the layered structure of the electrode, gel and relevant skin layers. The right side of the Figure shows the equivalent circuit model. In this circuit model, E_{hc} is the half-cell potential, representing the electrode–electrolyte interface when the wet electrodes are attached to the body [21]. Furthermore, this interface also has resistive and capacitive properties denoted by the resistor R_d and C_d. The resistance R_g placed in series represents the conductivity between the electrode and the skin, caused by the effects of the conductive gel. E_{se} is the potential created by a difference in ionic concentration across the stratum corneum and the conductive gel. R_e and C_e are the resistive and capacitive properties of the Epidermis layer. Finally, R_u represents the resistive properties of the Dermis layer. Its capacitive properties can be neglected.

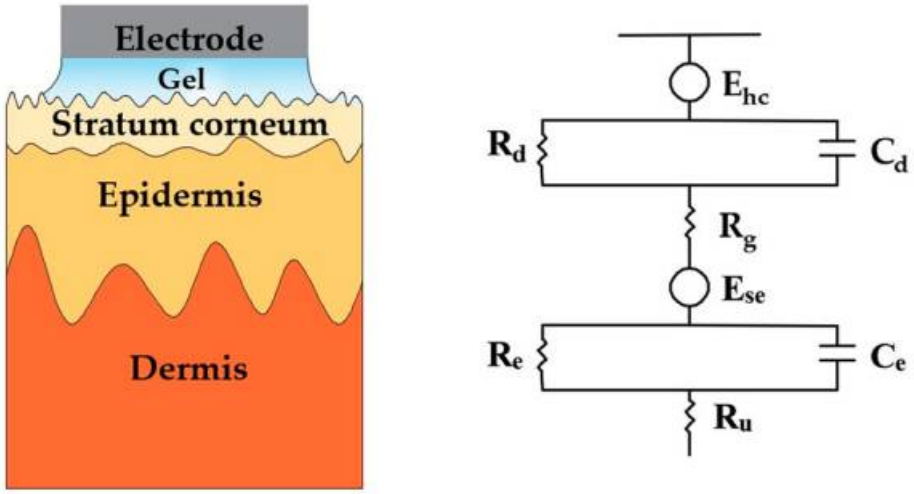

Figure 1.1: Schematic and electrical equivalent circuit model of electrode–skin interface for wet electrodes [19].

1.3.2. Dry Surface Electrodes

However, for this project, dry surface electrodes will be used. When using dry-contact electrodes, no conductive gel is applied between the electrodes and the skin. Instead, the instrumentation and electrodes are designed to accommodate and reduce the effect of variations in the electrode-skin interface[14].

The simplified equivalent circuit is now visualized by Figure 1.2. As there is no conductive gel applied, the resistance R_g and potential E_{se} are replaced by a resistance R_i and a capacitance C_i instead.

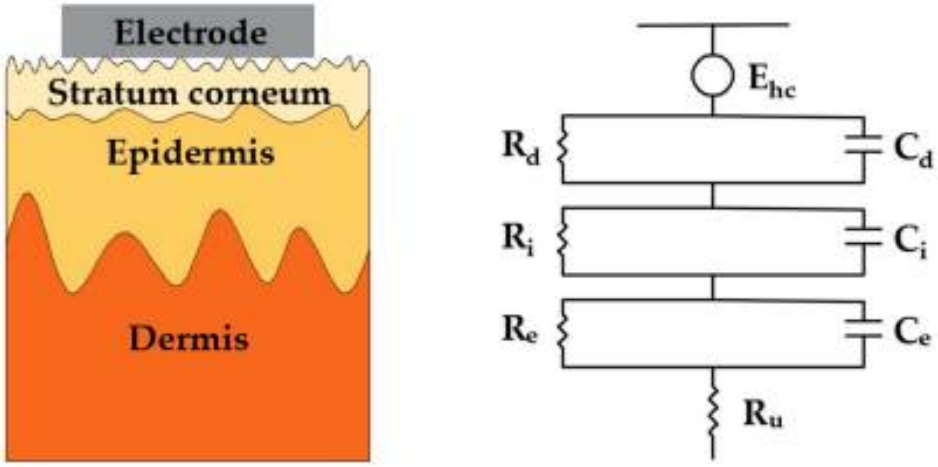

Figure 1.2: Schematic and electrical equivalent circuit model of electrode–skin interface for surface dry electrodes [19].

The produced set of dry surface electrodes to be used for this project consist of a CNT/PDMS (carbon nanotubes/polydimethylsiloxane) mix with a 4.5% wt [1]. Figure 1.3 shows the comparison of measured impedance of composite elastomers in response to different additives. It also gives the comparison of skin-electrode contact impedance when a wet electrode (Ag/AgCl) is used versus that of a dry electrode (AgNWs/CNTs/PDMS) [20].

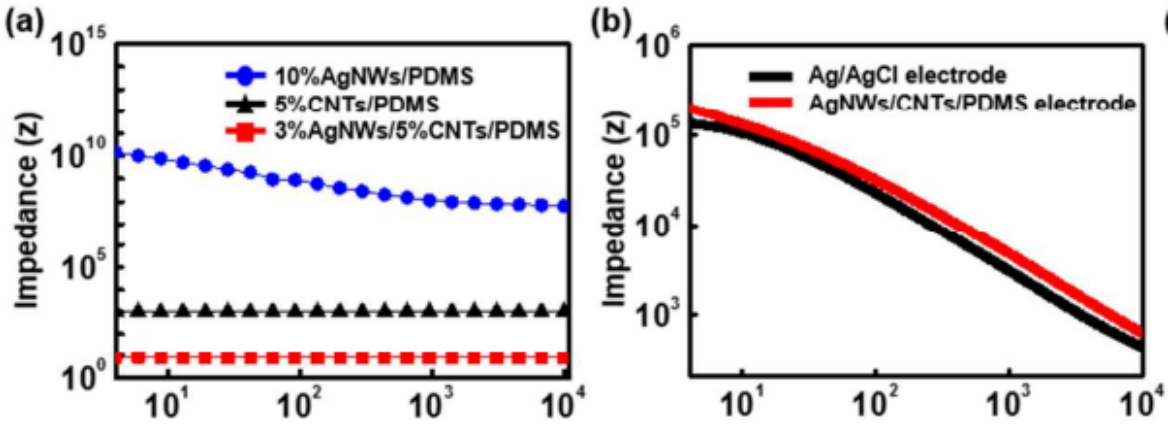

Figure 1.3: [20] (a) Comparison of measured impedance of composite elastomers in response to different additives. (b) Comparison of skin-electrode contact impedance when a wet electrode (Ag/AgCl) is used versus that of a dry electrode (AgNWs/CNTs/PDMS).

1.4. Cerumen and Electrodermal Response

It has been shown that the electrodermal activity and the concentration, location and natural flow of cerumen have a significant impact on the average dry-contact impedance in the ear canal [15]. The measured impedance increases up to 86% for higher concentrations of cerumen compared to canals removed of cerumen. Electrodermal activity shows a decrease in the impedance with up to 25%.
Besides, it has been shown that it is possible to simulate pores and sweat ducts by including microholes with a diameter and depth in the order of μm in the phantom structure [28].

1.5. Data acquisition

The dielectric measurements were performed using automatic swept-frequency network and impedance analysers. The frequency range 10 Hz to 10 MHz was covered by an HP4192A impedance analyser [5]. Open-ended co-axial probes were used to interface the measuring equipment with the samples. The probe is characterized by a fringing capacitance **C** and resistance **R** which are functions of its physical dimension and can be measured with the impedance analyser. The characteristic parameters of the probe, equivalent to its capacitance in air **K**, were calculated from measurements of the impedance components of the probe in air and in a standard sample (water or salt solution). In principle, the dielectric properties (permittivity ϵ' and conductivity σ) of an unknown sample could then be calculated from measurements of the impedance of the probe against an unknown sample using the following relationships [5]:

$$\epsilon' = \frac{C}{K} \tag{1.4}$$

$$\sigma = \frac{\epsilon_0}{RK} \tag{1.5}$$

From the conductivity σ, the out-of-phase loss factor ϵ" can be calculated by using Equation 1.2. Combining ϵ' with ϵ", the total complex permittivity can be derived using Equation 1.1.

1.6. Ear measurements

There are several ways to measure the dielectric constants and impedance of the skin, these are explained below:

1. Currently, the most commonly used skin complex permittivity measurement method involves measuring the reflection coefficient of skin in contact with an open-ended coaxial or a rectangular waveguide probe. Subsequently, the measured reflection coefficient is used in conjunction with an electromagnetic model that describes the measurement environment to extract the complex permittivity [22].

1.6.1. Process

The Voltage Network Analyzer (VNA) transmits an electromagnetic incident wave (incident signal) into the coaxial probe which is pressed against the tissue sample at one end and attached to the VNA at the other end. The incident signal (Vi$\angle\beta$) propagates into the probe and hits the sample at the probe-sample interface region where part of it reflects back to the VNA through the probe due to the impedance mismatch. This reflected wave (Vr$\angle\alpha$) affects the amplitude and phase of the incident wave (Vi$\angle\beta$) in the coaxial probe. By measuring and analyzing the phase and amplitude of the incident and reflected waves, the VNA estimates the sample's impedance. [25]

$$\Gamma = \frac{V_r\angle\alpha}{V_i\angle\beta} \tag{1.6}$$

This leads to:

$$Z_s = \frac{1+\Gamma}{1-\Gamma} Z_i \tag{1.7}$$

Where Γ is the reflection coefficient, V_r and α are the amplitude and phase angle of the reflected wave, V_i and β are the amplitude and phase angle of the incident wave. Z_i is the impedance of the coaxial probe and z_s is the impedance of the sample.

Based on Equation 1.6, at low frequencies where the impedance of biological tissues is significantly higher than the impedance of the coaxial probe, the reflection coefficient at the probe-sample interface becomes very close to 1, leading to a very large value. This implies that, at low frequencies, inevitable raw data measurement errors involved in the conventional permittivity measurement technique leads to highly magnified error in the sample permittivity estimation [25].

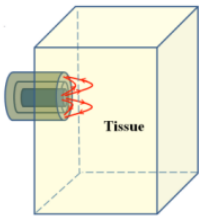

Figure 1.4: Coax probe against tissue sample

2. A freshly excised block-shaped tissue specimen is placed between two conductive plates. C is a physical property of the capacitor consisting of the two conductive plates and the tissue specimen sandwiched between them acting as the capacitor's dielectric. This parameter depends on the conductive plates' geometry and the tissue permittivity which is an intrinsic property of the tissue.
   So the permittivity of the dielectric can be calculated based on the dimensions of the plates and the measured capacitance. Practically, this cannot be done with living tissue since you need a standalone piece of tissue. This can however be done with dead homogeneous material such as gelatine.

It has been shown that there is a frequency dependent disagreement between the complex permittivity for different skin structures as well as a significant variation among test persons. To measure the complex relative permittivity of the hand palms and fingertips, a setup consisting of a vector network analyzer open-ended coaxial probe covering the right frequency spectrum can be used. The complex relative permittivity can then be obtained from the measured reflection coefficient by software. Important is to first calibrate the setup using the right procedure before each test [16].
It is handy to measure the charge present in the ear when the electrodes are active. It is necessary that there is an equal amount of charge being transmitted and received. If this is not the case, charge will build up in the ear and to much charge can destroy tissue. The skin-contact impedance can be measured using a impedance analyzer connected to a three-electrode setup. Besides the electrode under test, a reference and counter electrode are needed [12].

1.7. Electricity on skin behaviour

In order to evaluate the performance of the skin stimulation by the BCI experimentally, it is necessary to develop a phantom that appropriately mimics tissue [9]. Not only because of ethical reasons, but also to make representative measurements of the energy absorption induced in real human bodies. Using the dielectric properties of the skin, the exponential power decrease can be calculated as a function of depth, which then again determines the minimal thickness of the phantom. The attenuation of the power density and specific absorption rate are maximal at the skin interface. For a frequency of 60 GHZ, only a small percentage of 0.1% of the incident power reaches a skin depth of 1 mm.

2

Figures

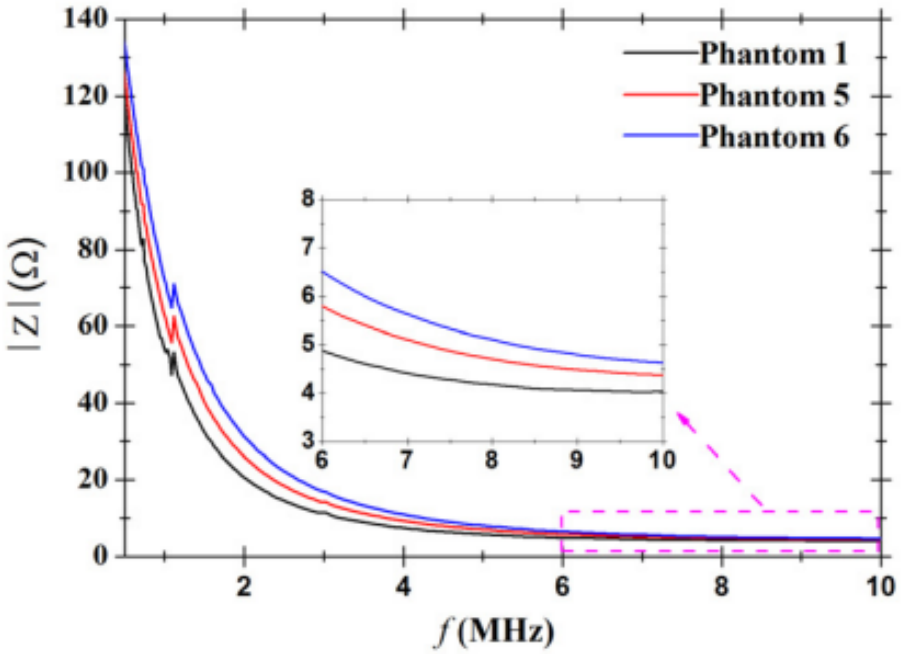

Figure 2.1: Impedance modulus as a function of the frequency, for phantoms with different gelatin contents.[2]

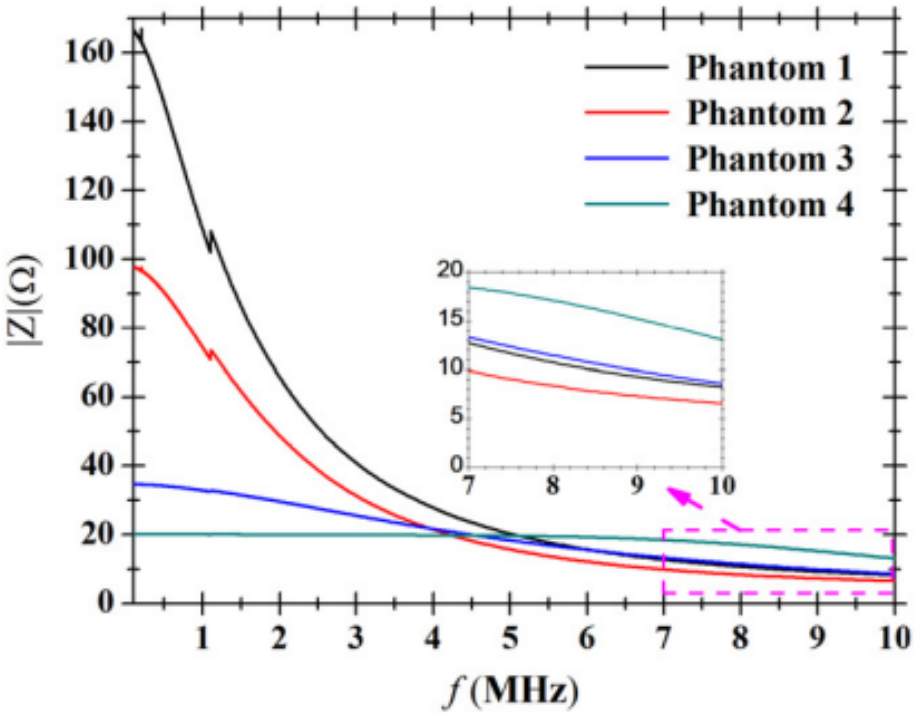

Figure 2.2: Impedance modulus as a function of the frequency, for phantoms with different salt content and 10% gelatin concentration.[2]

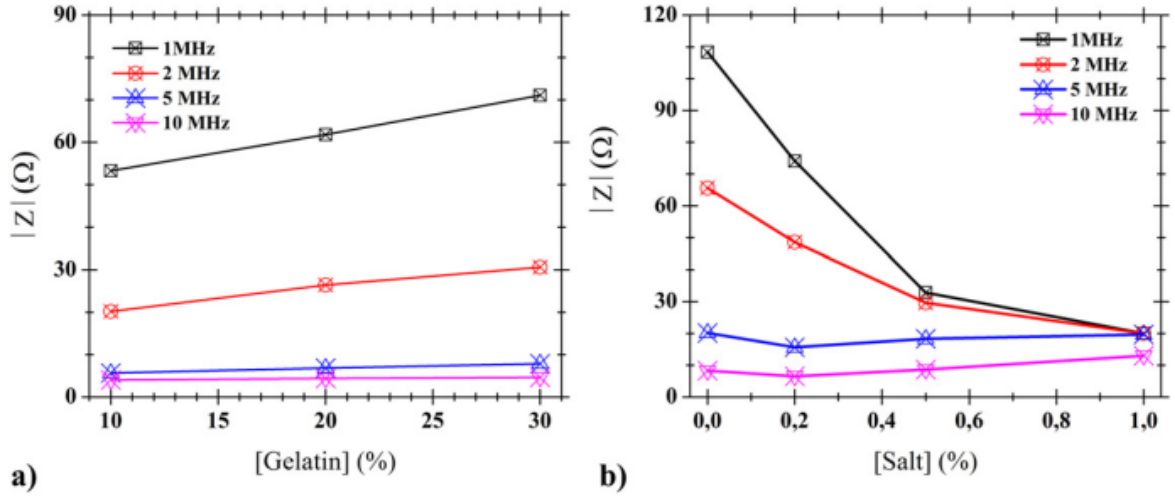

Figure 2.3: Impedance modulus as a function of(a) gelatin concentration and (b)salt concentration.[2]

Bibliography

[1] P. Burgar, *Progress update: Dry electrodes*, April 2022.

[2] A. M. R. Pinto, *Gelatin: a skin phantom for bioimpedance spectroscopy*, São Paulo, Brazil: Biomedical Physics & Engineering Express, 2015.

[3] A. Y. Owda, A. Casson, *Electrical properties, accuracy, and multi-day performance of gelatine phantoms for electrophysiology*, bioRxiv, May 2020.

[4] C. Gabriel, S. Gabriel and E Corthout, *The dielectric properties of biological tissues: I. Literature survey*, Phys. Med. Biol., vol. 41, no. 11, pp. 2271–2293, 1996.

[5] S. Gabriel, R. W. Lau and C. Gabriel, *The dielectric properties of biological tissues: II. Measurement in the frequency range 10 Hz to 20 GHz*, Phys. Med. Biol., vol. 41, no. 11, pp. 2251-2269, 1996.

[6] S. Gabriel, R. W. Lau and C. Gabriel, *The dielectric properties of biological tissues: III. Parametric models for the dielectric spectrum of tissues*, Phys. Med. Biol., vol. 41, no. 11, pp. 2271–2293, 1996.

[7] W. Franks, I. Schenker, P. Schmutz and A. Hierlemann, *Impedance Characterization and Modeling of Electrodes for Biomedical Applications*, IEEE Transactions on Biomedical Engineering, vol. 52, no. 17, July 2005.

[8] Y. M. Chi, T. Jung and G. Cauwenberghs, *Dry-Contact and Noncontact Biopotential Electrodes: Methodological Review*, IEEE Reviews in Biomedical Engineering, vol. 3, 2010.

[9] N. Chahat, M. Zhadobov and R. Sauleau, *Skin-Equivalent Phantom for On-body Antenna Measurements At 60 GHz*, Electronics Letters, vol. 48, no. 2, March 2012.

[10] N. Chahat, M. Zhadobov and R. Sauleau, *New Method for Determining Dielectric Properties of Skin and Phantoms at Millimeter Waves Based on Heating Kinetics*, Electronics Letters, vol. 48, no. 2, March 2012.

[11] W. J. Staab, W. Sjursen, D. Preves and T. Squeglia, *A one-size disposable hearing aid is introduced*, The Hearing Journal, vol. 53, no. 4, April 2000.

[12] F. Stauffer, M. Thielen, C. Sauter, S. Chardonnens, S. Bachmann, K. Tybrandt, C. Peters, C. Hierold and J. Vörös, *Skin Conformal Polymer Electrodes for Clinical ECG and EEG Recordings*, Healthcare Mater, vol. 7, 2018.

[13] S. L. Kappel and P. Kidmose, *Study of Impedance Spectra for Dry and Wet EarEEG Electrodes*, IEEE, 2015.

[14] S. L. Kappel, M. L. Rank, H. O. Toft, M. Andersen and P. Kidmose, *Dry-Contact Electrode Ear-EEG*, IEEE Transactions on Biomedical Engineering, vol. 66, no. 1, Jan 2019.

[15] A. Paul, S. R. Deiss, D. Tourtelotte, M. Kleffner, T. Zhang, and G. Cauwenberghs, *Electrode-Skin Impedance Characterization of In-Ear Electrophysiology Accounting for Cerumen and Electrodermal Response*, IEEE, 2019.

[16] S. S. Zhekov, O. Franek, and G. F. Pedersen, *Dielectric Properties of Human Hand Tissue for Handheld Devices Testing*, IEEE, 2019.

[17] U. Birgersson, E. Birgersson and S. Ollmar, *A methodology forextracting the electrical properties of human skin*, Manuscript submitted for publication in Physiol., Meas., 2012.

[18] U. Birgersson, E. Birgersson and S. Ollmar, *Estimating electrical properties and the thickness of skin with electrical impedance spectroscopy: Mathematical analysis and measurements* J Electr Bioimp, vol. 3, July 2012.

[19] Y. Fu, J. Zhao, Y. Dong and X. Wang, *Dry Electrodes for Human Bioelectrical Signal Monitoring*. Sensors (Basel, Switzerland) 2013 3651, 2020.

[20] J.H. Lee, J.Y. Hwang, J. Zhu, H.R. Hwang, S.M. Lee, H. Cheng, S.H. Lee, S.W. Hwang, *Flexible Conductive Composite Integrated with Personal Earphone for Wireless, Real-Time Monitoring of Electrophysiological Signs*, ACS Appl. Mater. Interfaces, 2018.

[21] D. C. Grahame, *The Electrical Double Layer and the Theory of Electrocapillarity*, Chemical Reviews. 41 (3): 441–501, July 1947.

[22] Y. Gao, M. Tayeb Ghasr, M. Nacy, R. Zoughi, *Towards Accurate and Wideband In Vivo Measurement of Skin Dielectric Properties*, Ieeexplore.ieee.org, February 2019.

[23] V. Raicu, *A simple theoretical and practical approach to measuring dielectric properties with an open-ended coaxial probe*. Meas. Sci. Technol, vol. 6. 410-414, 1995.

[24] V. Raicu et al, *A quantitative approach to the dielectric properties of the skin*, Phys. Med. Biol, vol. 45, L1-L4, 2000.

[25] S. Hesabgar, R. Jafari and A. Samani, *Accurate Technique for Measuring Electrical Permittivity of Biological Tissues at Low Frequencies and Sensitivity Analysis*, ResearchGate, 2018.

[26] H. Zhao, X. Xiao, and Q. Sun, *Identifying Electric Shock in the Human Body via α Dispersion*, IEEE Transactions on Power Delivery, Vol. 33, No. 3, June 2018.

[27] S. Grimnes, Ø. G. Martinsen, *Alpha-dispersion in human tissue*, Journal of Physics: Conference Series 224, 2010

[28] C. Liu, Y. Huang, S. Li, Y. Chen, W. Z. Wang, J. Yu, W. Shih, Microelectromechencial system-based biocompatible artificial skin phantoms Micro Nano Letters, vol. 14, Iss. 3, pp. 333–338, 2019